runaweera, R. Carter, G. Grau, K. N. Mendis, *Am. J. Trop. Med. Hyg.* **58**, 204 (1998).
10. This study was carried out in the village of Gonoa, Madang Province, Papua New Guinea, between 28 June and 27 August 1992 (*15*). Children ≥4 years old were enrolled following informed consent from parents or guardians. Clinical malaria and drug use was monitored by self-reporting. One child reporting fever was eliminated from the study. Only children with ≥50% compliance with sampling were used in analyses. Ethical clearance was granted by the Medical Research Advisory Committee of Papua New Guinea, who recommend that asymptomatic malaria infections should not be treated in order to allow natural, protective immunity to develop.
11. J. A. Cattani *et al.*, *Am. J. Trop. Med. Hyg.* **35**, 3 (1986).
12. Combined mean number of infectious bites per person per day for the two most prevalent species, *P. falciparum* and *P. vivax* [T. R. Burkot, P. M. Graves, J. A. Cattani, R. A. Wirtz, F. D. Gibson, *Bull. WHO* **65**, 375 (1987)].
13. Parasite species density was obtained from thick and thin blood smears. Smears were air-dried, thin smears were fixed in methanol, and both were stained in 4% Giemsa in sodium phosphate buffer (pH 7.2) for 45 min. Enumeration was per 200 leukocytes and counts were converted to parasites/μl of blood, assuming 8000 leukocytes/μl.
14. All samples were analyzed from children with ≥2 *P. falciparum* smear-positive samples or ≥4 *P. vivax* positives (*15*). Blood from finger pricks was collected in EDTA and stored at −70°C, then 20-μl volumes were transferred to filter paper for DNA extraction [S. Kyes, A. G. Craig, K. Marsh, C. I. Newbold, *Exp. Parasitol.* **77**, 473 (1993)]. *Plasmodium falciparum* genotypes were determined by size and sequence polymorphisms in PCR-amplified alleles of the *merozoite surface protein 2* (*Msp2*) gene [H. Babiker, L. Ranford-Cartwright, A. Sultan, G. Satti, D. Walliker, *Trans. R. Soc. Trop. Med. Hyg.* **88**, 328 (1994)]. *Plasmodium vivax* genotypes were determined by polymerase chain reaction–restriction fragment length polymorphism (PCR-RFLP) analysis [M. C. Bruce, M. R. Galinski, J. W. Barnwell, G. Snouou, K. P. Day, *Am. J. Trop. Med. Hyg.* **61**, 518 (1999)] of alleles at the *merozoite surface protein 3 alpha* (*Msp3α*) locus [M. R. Galinski *et al.*, *Mol. Biochem. Parasitol.* **101**, 131 (1999)].
15. M. C. Bruce *et al.*, *Parasitology*, in press.
16. Episodes were quantified by consecutive smear-positive time points for *P. vivax* and *P. malariae*. Consecutive or 6-day positive time points were used for *P. falciparum* to adjust for periodicity resulting from synchronous growth and sequestration [(*15*); A. Färnert, G. Snounou, I. Rooth, A. Björkman, *Am. J. Trop. Med. Hyg.* **56**, 538 (1997)].
17. M. J. Cox *et al.*, *Trans. R. Soc. Trop. Med. Hyg.* **88**, 191 (1994).
18. M. G. Bulmer, *Biometrics* **31**, 901 (1975); D. R. Fox and J. Ridsdill-Smith, *Oecologia* **103**, 435 (1995). Zero microscopy values were replaced with 1 in autocorrelation and Bulmer tests.
19. K. N. Brown, *Immunol. Lett.* **25**, 97 (1990).
20. D. Kwiatkowski, *Parasitol. Today* **11**, 206 (1995).
21. T. Staalsoe and L. Hviid, *Parasitol. Today* **14**, 177 (1998).
22. K. N. Brown and I. N. Brown, *Nature* **208**, 1286 (1965).
23. C. F. Ockenhouse *et al.*, *J. Infect. Dis.* **177**, 1664 (1998).
24. H. Wolda and B. Dennis, *Oecologia* **95**, 581 (1993).
25. We thank the people of Gonoa for their long-standing cooperation and the staff of the Papua New Guinea Institute of Medical Research, Madang, for their assistance. Supported by grants to K.P.D., D.W., and M.P.A. from the European Commission, by a grant to K.P.D. from the Wellcome Trust, by NIH grant AI24710 to J.W.B., and NIH grant AI37545 and World Health Organization/TDR grants (950440 and 910495) to M.R.G. M.C.B. was supported by The UK Medical Research Council and The Wellcome Trust. C.A.D. was supported by The Wellcome Trust.

27 July 1999; accepted 15 December 1999

Mutations in *SDHD*, a Mitochondrial Complex II Gene, in Hereditary Paraganglioma

Bora E. Baysal,[1]* Robert E. Ferrell,[2] Joan E. Willett-Brozick,[1] Elizabeth C. Lawrence,[2] David Myssiorek,[5] Anne Bosch,[6] Andel van der Mey,[7] Peter E. M. Taschner,[6] Wendy S. Rubinstein,[3] Eugene N. Myers,[4] Charles W. Richard III,[9] Cees J. Cornelisse,[8] Peter Devilee,[6] B. Devlin[1]

Hereditary paraganglioma (PGL) is characterized by the development of benign, vascularized tumors in the head and neck. The most common tumor site is the carotid body (CB), a chemoreceptive organ that senses oxygen levels in the blood. Analysis of families carrying the *PGL1* gene, described here, revealed germ line mutations in the *SDHD* gene on chromosome 11q23. *SDHD* encodes a mitochondrial respiratory chain protein—the small subunit of cytochrome b in succinate-ubiquinone oxidoreductase (cybS). In contrast to expectations based on the inheritance pattern of PGL, the SDHD gene showed no evidence of imprinting. These findings indicate that mitochondria play an important role in the pathogenesis of certain tumors and that cybS plays a role in normal CB physiology.

Regulation of oxygen homeostasis is essential for most organisms (*1*). In mammals, the CB, a highly vascular small organ located at the bifurcation of the common carotid artery in the neck, plays a major role in acute adaptation to hypoxia (oxygen deprivation) by stimulating the cardiopulmonary system (*2*). At the cellular level, this adaptation involves activation of a transcription factor, hypoxia-inducible factor–1 (HIF-1), which subsequently leads to a systemic response, including an increase in red blood cell mass, stimulation of new blood vessel growth, and increased ventilation (*3*). Chronic exposure to hypoxia (e.g., as occurs in individuals dwelling at high altitudes or in those with certain medical conditions, such as cyanotic heart and chronic lung diseases) induces cellular hyperplasia/anaplasia in the CB (*4*).

The CB is also the most common tumor site for hereditary paraganglioma (PGL), a rare disorder characterized by the development of mostly benign, highly vascular, slow-growing tumors in the head and neck. PGL tumors display cellular hyperplasia/anaplasia (*5*) in the absence of any hypoxic stimulus. A gene responsible for PGL was mapped to chromosome band 11q23 (*PGL1*) and remains the only locus confirmed in independent families (*6–8*). *PGL1* is inherited in an autosomal dominant fashion with incomplete penetrance when transmitted through fathers, whereas no disease phenotype occurs when transmitted maternally. This inheritance pattern is observed in all confirmed *PGL1* pedigrees and suggests that there is sex-specific epigenetic modification of *PGL1* during gametogenesis, consistent with genomic imprinting (*9*). This consistent inheritance pattern gives PGL a unique place among the known human genetic disorders with parent-of-origin effects (*10*). Several features of PGL tumors, including their benign biological behavior, limited organ involvement, and histopathology, are markedly similar to those of chronic hypoxia-stimulated CBs. This led us to hypothesize that the genetic defect in *PGL1* involves a critical component in the oxygen-sensing and -signaling pathway.

We previously localized *PGL1* to an approximately 1.5-Mb critical interval between D11S1986 and D11S1347 (*8*). BAC and yeast artificial chromosome (YAC) contig construction and discovery of 16 new simple tandem repeat polymorphisms (STRPs) (*11*) enabled us to confine *PGL1* to an approximate 400-kb region (*12*) flanked by the recombination breakpoints in families 5 (*7*) and 12 (*8*) (Fig. 1).

Expressed sequence tag (EST) gene content mapping of transcripts (*13*) revealed a high density of transcripts in the 400-kb *PGL1* critical region and in its close vicinity (*11*). A database search using BLAST with one of the ESTs in the critical region,

[1]Department of Psychiatry, [2]Department of Human Genetics, [3]Pittsburgh Cancer Institute, [4]Department of Otolaryngology, The University of Pittsburgh Medical Center, Pittsburgh, PA 15213–2593, USA. [5]Department of Otolaryngology and Communicative Disorders, Long Island Jewish Medical Center, New Hyde Park, New York, NY 11040, USA. [6]Department of Human Genetics, [7]Department of Otolaryngology, [8]Department of Pathology, Leiden University Medical Center, 2300 RA, Leiden, Netherlands. [9]Wyeth-Ayerst Research, Genetics Institute, 35 Cambridgepark Drive, Cambridge, MA 02140, USA.

*To whom correspondence should be addressed. E-mail: baysalbe@msx.upmc.edu

EST229158 (*14*), identified a complete match to a genomic sequence (GenBank accession number AB026906) containing the exons of the succinate-ubiquinone oxidoreductase subunit D gene (*SDHD*). *SDHD* was previously mapped to chromosome band 11q23 by fluorescence in situ hybridization (FISH) (*15*) and its genomic structure has been characterized (*16*). We confirmed the location of *SDHD* in the *PGL1* critical region by mapping it back to the BAC and YAC contigs, and placed it close to the telomeric exclusion border. *SDHD* spans over 19 kb at the genomic level, and its translated region consists of four exons of 52, 117, 145, and 163 base pairs (bp).

SDHD encodes the small subunit (cybS) of cytochrome b in succinate-ubiquinone oxidoreductase (mitochondrial complex II). Mitochondrial complex II is involved in the Krebs cycle and in the aerobic electron transport chain (*17*). It contains four proteins. The catalytic core consists of a flavoprotein and an iron-sulfur protein; these proteins are anchored to the mitochondrial inner membrane by the large subunit of cytochrome b (cybL) and cybS, which together comprise the hemeprotein cytochrome b (*18*).

Because it has been postulated that the mitochondrial electron transport chain plays a critical role in oxygen sensing and signaling (*19*), we evaluated *SDHD* as a candidate gene for PGL1. To test for germ line mutations in *SDHD*, we initially selected five families (families 3, 5, 7, 8, and 11) who showed significant linkage to *PGL1* and demonstrated distinct disease haplotypes (*7*, *8*). Using two affected or carrier individuals from each family, we amplified each exon and its splice sites by primers designed from the flanking intronic sequences and subjected each amplicon to single-strand conformational polymorphism (SSCP) analysis (*20*). The SSCP analysis yielded at least one aberrant conformer that cosegregated with the disease chromosome in each family. Families 5 and 7 had the same aberrant conformer, whereas family 3 had a distinct aberrant conformer in exon 3. Family 11 had an aberrant conformer in exon 2 and family 8 showed distinct aberrant conformers in exons 2 and 3.

Direct sequencing of each amplicon revealed the sequence alterations responsible for the SSCP conformers (Fig. 2). Families 8 and 11 have nonsense mutations at codon 36 and codon 38, respectively, creating premature stop codons. Both stop codons are located within the mitochondrial signal peptide and presumably block production of mature cybS. Family 3 has a missense mutation, changing $His^{102} \rightarrow Leu^{102}$. Families 5 and 7 have a missense mutation that changes $Pro^{81} \rightarrow Leu^{81}$. We previously described extensive haplotype sharing among families 12, 24, and 26 (*8*). These families also show extensive haplotype sharing with family 7 and, as expected, they all have the same missense mutation. Finally, direct sequencing of *SDHD* from individuals who carry the Dutch founder mutation (*21*) revealed a missense mutation that changes $Asp^{92} \rightarrow Tyr^{92}$. All of the missense mutations replace amino acids conserved in four eukaryotic multicellular organisms (Fig. 3). His^{102} is located in a region thought to harbor an axial ligand for heme in the *Escherichia coli* enzyme (*22*). The other two missense mutations result in nonconservative amino acid substitutions that could dramatically alter cybS conformation. None of the mutations has been observed in more than 200 normal control chromosomes. The mutations cosegregate with the disease phenotype in all affected individuals. The mutations are also inherited in a Mendelian fashion by all at-risk (paternal inheritance) and not-at-risk (imprinted maternal inheritance) carrier individuals as identified by haplotype analysis.

We assessed allele-specific expression of *SDHD* to determine whether the lack of maternal disease transmission in *PGL1* is caused by paternal monoallelic imprinted gene expression. We detected biallelic expression (*23*) in lymphoblastoid cell lines from affected and imprinted carrier individuals and in adult brain tissue as well as in fetal tissues from the brain and kidney (Fig. 4). Thus these results cannot explain why children of affected mothers do not develop PGL. Unlike most endogenously imprinted genes, *SDHD* is not located in an imprinted genomic domain (*24*). This observation has prompted the hypothesis that *PGL1* mutations cause ectopic imprinting (*7*, *8*). Given the single base pair mutations in *SDHD* and its biallelic expression in lymphoblastoid cells from affected and imprinted individuals, this hypothesis seems unlikely. Although the precise mecha-

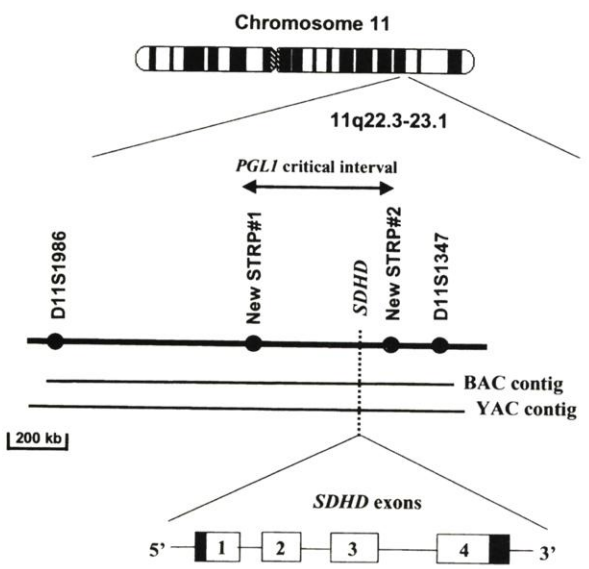

Fig. 1 (left). A summary map of the *PGL1* critical region on chromosome 11q23. Two new STRPs confined the critical region to approximately 400 kb. *SDHD* was localized within the critical region with a BAC and YAC contig. The genomic structure of *SDHD* is shown schematically at the bottom but is not drawn to scale. Exons are denoted with boxes; introns are denoted with horizontal lines. The solid boxes in exons 1 and 4 represent the 5′– and 3′–untranslated regions, respectively.

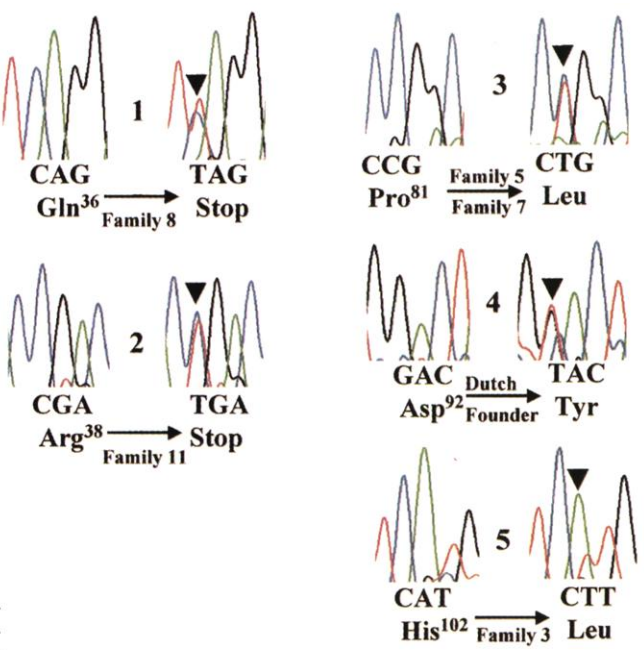

Fig. 2 (right). The sequencing chromatograms show the alterations (denoted with arrowheads) responsible for the five major *PGL1* mutations. The affected codons and the amino acids are depicted below the chromatograms.

nism of the imprinted inheritance pattern in *PGL1* remains to be determined, monoallelic expression of *SDHD* may be confined to the CB and other paraganglionic cells, similar to the brain-limited imprinting of *UBE3A* of Angelman syndrome (*25*).

Tumors from *PGL1* families often show loss of heterozygosity with exclusive loss of the normal maternal chromosome at 11q23 (*7*, *26*). Our analysis of 11 hereditary tumors, nine of which were informative at STRPs within 500 kb of *SDHD*, confirmed loss of maternal alleles in all nine cases. In four cases, including the two uninformative ones, the availability of highly enriched tumor cell populations by fluorescence-activated cell sorting allowed us to demonstrate that the mutated allele of *SDHD* was retained and that the normal wild-type *SDHD* allele was completely lost in the tumor (*27*). Germ line loss-of-function mutations in the paternal alleles and subsequent somatic loss of normal maternal alleles suggest that *SDHD* functions as a tumor suppressor gene at the cellular level and needs two events for inactivation. PGL is unusual among hereditary tumor syndromes in that the defective gene encodes a mitochondrial protein. The growth advantage conferred by the loss of maternal chromosomes indicates that imprinting is not absolute in the normal CB or that there is secondary relaxation of imprinting at the maternal allele during tumorigenesis.

On the basis of the phenotypic similarity between PGL tumors and the normal CB exposed to chronic hypoxia, we hypothesize that cybS is a critical component of the oxygen-sensing system of paraganglionic tissue, and that its loss may lead to chronic hypoxic stimulation and cellular proliferation. Hypoxic stimulation has also been implicated as an etiologic factor in von Hippel–Lindau disease tumors, where there is constitutive activation of HIF-1 (*28*). It is well known that solid tumors are hypoxic relative to normal tissue. This hypoxia not only affects gene expression patterns but it can also be an important prognostic factor and may make tumors resistant to radiation and certain forms of chemotherapy (*29*). Thus, hypoxic stimulation may provide a selective advantage for tumor cells (*30*). Interestingly, the *SDHD*-containing region on chromosome 11q23 (*7*) is a common site of somatic deletions in bladder, breast, cervical, stomach, lung, ovary, and nasopharyngeal carcinomas, as well as melanoma (*31*). Identification of *SDHD* as the gene responsible for PGL will likely increase our understanding of tumorigenesis and may also have future therapeutic potential.

```
                                                       1 2
H.sapiens        MAVLWRLSAVCGALGGRALLLRTPVVR---PAHISAFLQDRPIPEWCGVQHIHLSPSHHS
B.taurus         -MALWRLSVLCGAKEGRALFLRTPVVR---PALVSAFLQDRPAQGWCGTQHIHLSPSHHS
A.suum           -----MLSAVRRAIPLSARILRTSLIQRCAGATSAAVTGAAPPQFDPIAAEKGFKPLHSH
C.elegans        ---------MAASLRHMAHFQKALLVAR--SAPRISTIVRATSTLNDGASKV---PDHS-
                                  *             *                       * *

                                        3          4         5
H.sapiens        GSKAASLHWTSERVVSVLLLGLLPAAYLNPCSAMDYSLAAALTLHGHWGLGQVVTDY---
B.taurus         GSKAASLHWTGERVVSVLLLGLIPAAYLNPCSAMDYSLAATLTLHSHWGIGQVVTDY---
A.suum           GT-----LFKIERYFAAAMVPLIPAAYFIHGREMDLCLALALTLHVHWGVWGVVNDYGRP
C.elegans        ------MHFKLERLWAVGMLPILPASYFIHGPVMDAVLTVALTLHIHWGIHGVVYDYARP
                            **          ** *      **  *   **** ***   ** **

H.sapiens        -VHGDALQKAAKAGLLALSALTFAGLCYFNYHDVGICKAVAMLWKL
B.taurus         -VHGDAVQKAAKTGLLVLSAFTFAGLCYFNYHDVGICKAVAMLWKL
A.suum           FVLGDTLAAAVRVGAYIFTACLLAGLLYFNEHDVGLTRAFEMVWEL
C.elegans        YVIGEAAAKAAHVGVYLITGLLLGALLHFNTNDVGITKAFELVFSL
                  * *     *   *           *  **  ***   *      *
```

Fig. 3. Alignment of cybS amino acid sequences from *Homo sapiens*, *Bos taurus* (domestic cattle), *Ascaris suum* (a parasitic nematode), and *Caenorhabditis elegans*, identified by BLASTP analysis of the Swissprot database, revealed conserved amino acids (denoted with asterisks) and was performed with Clustalw 1.7 (available at www.medkem.gu.se/ln/molbio/gene/msf.html). The numbers indicate the mutated amino acids (in bold) in PGL families (Fig. 2) (*32*). The horizontal bars denote the amino acids with codons spanning exon-exon boundaries in the human genomic sequence. The vertical arrow denotes the amino terminus of the mature cybS.

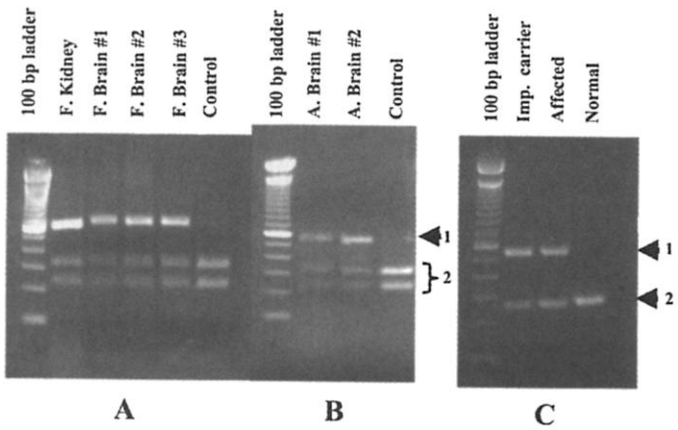

Fig. 4. Biallelic expression of human *SDHD*. (**A**) Three independent fetal brain samples and one fetal kidney sample show expression of both alleles as detected by RT-PCR–restriction enzyme digestion analysis with Spe I. A homozygous brain sample is included in the right lane as a control for restriction enzyme digestion. (**B**) Two independent adult brain samples show biallelic expression. The method is the same as described in (A). A homozygous sample is included in the right lane as a control for restriction enzyme digestion. The numerals 1 and 2 at right denote the two alleles distinguished by the restriction enzyme digestion. (**C**) Lymphoblastoid cell lines from both PGL-affected and -imprinted carriers show biallelic expression. The mutation in family 5 was used for RT-PCR–restriction enzyme digestion analysis with Msp I. A lymphoblastoid cell line from a normal individual is included in the right lane as a control for restriction enzyme digestion. The mutant and the normal alleles are denoted at right by the numerals 1 and 2, respectively.

References and Notes

1. H. Zhu and H. F. Bunn, *Respir. Physiol.* **115**, 239 (1999); G. L. Semenza, *Cell* **98**, 281 (1999); H. F. Bunn and R. O. Poyton, *Physiol. Rev.* **76**, 839 (1996).
2. C. Gonzalez, L. Almaraz, A. Obeso, R. Rigual, *Physiol. Rev.* **74**, 829 (1994).
3. It has been postulated that adaptation to hypoxia involves activation of the transcription factor HIF-1. Normoxic conditions lead to oxidative modification and degradation of the alpha subunit of HIF-1, preventing the activation of HIF-1. The activated HIF-1 stimulates the synthesis of erythropoietin (Epo), which increases red blood cell mass; of vascular endothelial growth factor, which stimulates new blood vessel growth; and of tyrosine hydroxylase, which is involved in the control of ventilation by the CB (*1*, *2*).
4. J. Arias-Stella and F. Bustos, *Arch. Pathol. Lab. Med.* **100**, 636 (1976); J. Arias-Stella and J. Valcarcel, *Hum. Pathol.* **7**, 361 (1976); C. Edwards *et al.*, *J. Pathol.* **104**, 231 (1971); M. J. Saldana, L. E. Salem, R. Travezan, *Hum. Pathol.* **4**, 251 (1973); L. Morelli, C. Di Giulio, M. Iezzi, P. G. Data, *Sci. Total Environ.* **150**, 215 (1994); D. Bee, D. J. Pallot, G. R. Barer, *Acta Anat.* **126**, 226 (1986); C. A. Nurse and C. Vollmer, *Dev. Biol.* **184**, 197 (1997); E. E. Lack, *Am. J. Pathol.* **91**, 497 (1978); E. E. Lack, A. R. Perez-Atayde, J. B. Young, *Am. J. Pathol.* **119**, 301 (1985).
5. E. E. Lack, A. L. Cubilla, J. M. Woodruff, *Hum. Pathol.* **10**, 191 (1979); D. Stiller, D. Katenkamp, K. Kuttner, *Virchows Arch. A Pathol. Anat. Histol.* **365**, 163 (1975).
6. P. Heutink *et al.*, *Hum. Mol. Genet.* **1**, 7 (1992); P. Heutink *et al.*, *Eur. J. Hum. Genet.* **2**, 148 (1994); J. Milunsky *et al.*, *Am. J. Med. Genet.* **72**, 66 (1997).
7. B. E. Baysal *et al.*, *Am. J. Hum. Genet.* **60**, 121 (1997).
8. B. E. Baysal *et al.*, *Hum. Genet.* **104**, 219 (1999).
9. A. G. van der Mey, P. D. Maaswinkel-Mooy, C. J. Cornelisse, P. H. Schmidt, J. J. van de Kamp, *Lancet* **2**, 1291 (1989).
10. I. M. Morison and A. E. Reeve, *Hum. Mol. Genet.* **7**, 1599 (1998).
11. B. E. Baysal *et al.*, in preparation.
12. The polymerase chain reaction (PCR) primer sequences for the two new CA repeat polymorphisms, that flank the 400-kb critical interval size were as follows: STRP1 (D11S5011), 5′-TTGGCATCAATGGAAAGCACT-3′ and 5′-TTGGGAATCTTTTGCCTGGAA-3′; STRP2 (D11S5019), 5′-CATTTGTCCAGTTACCCGTA-3′ and 5′-TATTGACTAATGGACACTGGAA-3′. STRP1 has five alleles in the 187- to 195-bp range. STRP2 has four alleles in the 168- to 174-bp range. Both STRP were amplified with standard PCR conditions (*20*) and analyzed as described (*7*).

13. B. E. Baysal *et al.*, *Genomics* **44**, 214 (1997); P. Deloukas *et al.*, *Science* **282**, 744 (1998).
14. The complete sequence of EST229158 is available at the Genome Database (http://gdbwww.gdb.org/).
15. H. Hirawake, M. Taniwaki, A. Tamura, S. Kojima, K. Kita, *Cytogenet. Cell Genet.* **79**, 132 (1997).
16. H. Hirawake *et al.*, *Biochim. Biophys. Acta* **1412**, 295 (1999).
17. I. E. Scheffler, *Prog. Nucleic Acid Res. Mol. Biol.* **60**, 267 (1998).
18. cybL is also known as QPs-1 or $C_{II,3}$, and cybS is also known as QPs-3 or $C_{II,4}$.
19. N. S. Chandel *et al.*, *Proc. Natl. Acad. Sci. U.S.A.* **95**, 11715 (1998).
20. The primers for exon amplifications were as follows: 1F, 5′-TGACCTTGAGCCCTCAGGAACG-3′ and 1R, 5′-TCAGGGTGGGAAGACCCCT-3′; 2F, 5′-GATCATCCTAATGACTCTTTCC-3′ and 2R, 5′-AGCAGCAGCGATGGAGAGAA-3′; 3F, 5′-CTTTTATGAATCTGGTCCTTTTTG-3′ and 3R, 5′-CAACTATATTTGGAATTGCTATAC-3′; 4F, 5′-TGATGTTATGATTTTTTCTTTTTCT-3′ and 4R, 5′-CAATTCTTCAAAGTATGAAGTCA-3′. Primers 1F and 4R are located in 5′ and 3′ untranslated regions in exons 1 and 4, respectively. The other primers were designed from intronic sequences. The amplicon sizes for exons 1, 2, 3, and 4 are 98 bp, 168 bp, 200 bp, and 224 bp, respectively. PCR amplifications of 50 to 100 ng of genomic DNA were performed in Techne PHC3 thermal cyclers using AmpliTaq Gold DNA polymerase (Perkin Elmer Cetus). Amplification conditions were as follows: initial denaturation at 94°C for 10 min, then 35 cycles of 45 s of denaturation at 94°C, 45 s of annealing at 55°C, and 45 s of extension at 72°C, and completed with a final extension at 72°C for 10 min. The amplicons were first visualized in a 1% ethidium bromide–stained agarose gel. SSCP analysis was performed with genomic DNA as described [B. E. Baysal, J. Farr, J. Goss, B. Devlin, C. W. Richard III, *Gene* **217**, 107 (1998)]. Aberrant amplicons were sequenced in an ABI377 fluorescent sequencer. The segregation of mutations in PGL families and screening in normal control chromosomes were performed by restriction enzyme analyses of mutant amplicons. The mutations in PGL families result in loss of the recognition site for the following restriction enzymes: family 3, Nla III; family 5 and family 7, Msp I; family 8, Mbo II; family 11, Ava II. The Dutch founder mutation results in gain of an Rsa I site.
21. E. M. van Schothorst *et al.*, *Am. J. Hum. Genet.* **63**, 468 (1998).
22. K. Nakamura *et al.*, *J. Biol. Chem.* **271**, 521 (1996); C. R. Vibat, G. Cecchini, K. Nakamura, K. Kita, R. B. Gennis, *Biochemistry* **37**, 4148 (1998); S. K. Shenoy, L. Yu, C. Yu, *J. Biol. Chem.* **274**, 8717 (1999).
23. The single-step method of RNA extraction [P. Chomczynski and N. Sacchi, *Anal. Biochem.* **162**, 156 (1987)] was used according to a commercial protocol (RNAzol B, Tel-Test, Friendswood, TX). Complementary DNA synthesis was performed using SUPERSCRIPT II (Life Technologies) and oligo(dT) primers; the recommended conditions were used. Reverse transcriptase–PCR (RT-PCR) of cDNA templates was performed by 30 to 35 cycles of amplification with primers 1F and 4R (amplicon size, 533 bp). PCR products were precipitated with isopropanol, washed with 70% ethanol, and resuspended in tris-EDTA buffer. A synonymous single nucleotide polymorphism (SNP)—(C/T) in codon 68 in exon 3—was identified by SSCP and sequence analysis in family 8 and in several normal control samples. This SNP, detected by Spe I restriction enzyme digestion, was used for allelic expression analysis.
24. J. E. Farr *et al.*, *Am. J. Hum. Genet.* **65**, A271 (1999).
25. T. H. Vu and A. R. Hoffman, *Nature Genet.* **17**, 12 (1997).
26. P. Devilee *et al.*, *Genes Chromosomes Cancer* **11**, 71 (1994); E. M. van Schothorst *et al.*, *Hum. Pathol.* **29**, 1045 (1998).
27. P. Devilee *et al.*, data not shown.
28. P. H. Maxwell *et al.*, *Nature* **399**, 271 (1999).
29. P. Vaupel, O. Thews, D. K. Kelleher, M. Hoeckel, *Strahlenther. Onkol.* **174**, Suppl. 4, 6 (1998).
30. T. G. Graeber *et al.*, *Nature* **379**, 88 (1996).
31. J. Koreth, C. J. Bakkenist, J. O. McGee, *J. Pathol.* **187**, 28 (1999) and references therein.
32. Abbreviations for the amino acid residues are as follows: A, Ala; C, Cys; D, Asp; E, Glu; F, Phe; G, Gly; H, His; I, Ile; K, Lys; L, Leu; M, Met; N, Asn; P, Pro; Q, Gln; R, Arg; S, Ser; T, Thr; V, Val; W, Trp; Y, Tyr.
33. We thank the families participating in this study; R. Carrau, J. Johnson, A. Petropoulos, S. Farb, L. Coia, K. Grant, J. Nasser, J. Green, J. Kohn, D. Saphier, L. Pratt, W. Chase, J. Oosterwijk, M. Godfrey, S. Kirkpatrick, P. Heutink, S. Saha, and J. Jansen for referring patients; C. Melvin-Drovdlic for help in family counseling; J. Goss, U. Surti, S. Gollin, and N. Kuipers-Dijkshoorn for technical help; and G. J. B. van Ommen and D. Kupfer for administrative and financial support. Supported by grants from the University of Pittsburgh Medical Center (Competitive Medical Research Fund to B.E.B.), the American Cancer Society (VM-180), and the National Institute of Mental Health (MH57881) to B.D., and the Dutch Cancer Society (KWF98-1721 to A.B. and P.E.M.T.).

6 October 1999; accepted 13 December 1999

Honeybee Navigation: Nature and Calibration of the "Odometer"

Mandyan V. Srinivasan,[1]* Shaowu Zhang,[1] Monika Altwein,[2] Jürgen Tautz[2]

There are two theories about how honeybees estimate the distance to food sources. One theory proposes that distance flown is estimated in terms of energy consumption. The other suggests that the cue is visual, and is derived from the extent to which the image of the world has moved on the eye during the trip. Here the two theories are tested by observing dances of bees that have flown through a short, narrow tunnel to collect a food reward. The results show that the honeybee's "odometer" is visually driven. They also provide a calibration of the dance and the odometer in visual terms.

It is well known that honeybees navigate accurately and repeatedly to a food source, as well as communicate to their nestmates the distance and direction in which to fly to reach it, through the "waggle dance" (*1*). However, the cues by which bees gauge the distance to the goal have been controversial. Early work suggested that flight distance is estimated in terms of energy consumption (*2*). More recent studies suggest that the primary cue is the integral, over time, of the image motion that is experienced en route (*3*–*6*). Here we put the two theories to a stringent test by recording dances of bees that have been trained to fly into a short, narrow tunnel to collect a food reward.

The experimental bees (*Apis mellifera ligustica* Spinola) were housed in a two-frame observation hive, with transparent walls on both sides. One frame was positioned above the other so that all comb faces were visible for observing and filming dances. The hive was located on the inside wall of a building, with an exit to the outside. Typically, six bees were individually marked and used for each experiment.

In one series of experiments, individually marked bees were trained to forage at a feeder carrying sugar solution placed in a wooden tunnel 6.4 m long, 11 cm wide, and 20 cm high. The tunnel was positioned outdoors near the hive. The far end was closed, and bees could enter and leave the tunnel only at the near end. The top of the tunnel was covered with black insect-screen cloth, which permitted observation and provided the bees with a view of the sky.

In experiment 1, the tunnel was positioned with its entrance 35 m from the hive, and was oriented along the direction to the hive (Fig. 1A). The walls and floor of the tunnel were lined with a random visual texture (*7*). The feeder was placed at the entrance to the tunnel. Bees returning from the feeder performed predominantly round dances: The probability of a round dance was 85.2% (Fig. 1B). This is consistent with the fact that *A. mellifera ligustica* performs mainly round dances when visiting food sources that are within 50 m of the hive (*8*). However, when the feeder was placed 6 m inside the tunnel (experiment 2), the bees performed primarily waggle dances: The probability of a waggle dance was 90.0% (Fig. 1B) (*9*). This change from round dances to waggle dances occurred while the distance flown by the bees had increased by a mere 6 m, from 35 m in experiment 1 to 41 m in experiment 2. Clearly, in experiment 2, the feeder was still at a distance at which bees normally perform round dances when flying outdoors.

Why were the bees performing waggle dances in experiment 2? One possibility is that flight in the narrow tunnel generated a large integrated optic flow on the eye, mim-

[1]Centre for Visual Science, Research School of Biological Sciences, Australian National University, Canberra, ACT 2601, Australia. [2]Biozentrum, Universität Würzburg, Am Hubland, D-97074 Würzburg, Germany.

*To whom correspondence should be addressed. E-mail: M.Srinivasan@anu.edu.au